

Matthew Blandin¹ Hyunju Connor^{1,2} Doğaçon Öztürk¹ Amy Keese³ Victor Pinto³ MD Shaad Mahmud⁴ Chigomezyo Ngwira⁵ Shishir Priyadarshi⁶

¹Department of Physics and Geophysical Institute University of Alaska Fairbanks, ²NASA Goddard Space Flight Center, ³Department of Physics and Astronomy and Space Science Center University of New Hampshire Durham, ⁴Department of Electrical and Computer Engineering University of New Hampshire Durham, ⁵ASTRA Boulder CO, ⁶Department of Electronics and Electrical Engineering University of Bath

Key Points

- We develop a multi-variate LSTM code that predicts magnitude of north-south component of geomagnetic fields ($|B_N|$) using 15 years of SuperMAG Alaska Magnetometer data and OMNI solar wind data.
- Multivariate LSTM prediction shows reasonable agreement with geomagnetic field observations with high correlation coefficients.
- A secondary model to predict a sign of ($|B_N|$), named a polarity model, was trained for each station with an average HSS of 0.92.
- A coupled model, created by combining both models of $|B_N|$ and a sign of B_N , shows promising results to predict B_N as a function of solar wind and IMF conditions.

Introduction

Geomagnetically induced currents (GICs) are produced when the solar wind interacts with the Earth's magnetic field, driving disturbances that map to the Earth's surface. Electrically conductive materials like the Earth's crust, in the presence of these disturbances, experience electric fields proportional to that of the changing geomagnetic field which are known as geomagnetically induced electric fields (GIEs). These GIEs, if strong enough, produce currents in exposed electronics on the ground that can disrupt and damage components. GICs have been known to cause power outages, transformer damage, and pipeline corrosion on the ground which impacts our technology and fossil fuel dependent economy; such an event was the cause for a 9 hour power grid blackout in Quebec, Canada on 13 March, 1989, where strong GICs overloaded and damaged a transformer of the Hydro-Quebec electric company.

Acknowledgements

This work was supported by NSF EPSCoR Award OIA-1920965.

We acknowledge use of NASA/GSFC's Space Physics Data Facility's OMNIWeb service and OMNI data. We also acknowledge King et al. (2005) for their work on higher resolution OMNI datasets.

The results presented in this paper rely on the data collected at CMO (College, AK), FYU (Fort Yukon, AK), PKR (Poker Flat, AK), and KAV (Kaktovik, AK). We thank USGS (www.usgs.gov) and the Geophysical Institute (www.gi.alaska.edu) for supporting their continued operation and INTERMAGNET for promoting high standards of magnetic observatory practice (www.intermagnet.org).

We acknowledge superMAG and the work done by Gjerloev (2012) bringing a comprehensive worldwide magnetometer database which was utilized in this research. Magnetometer data, Geophysical Institute, UAF 2000-2015. Retrieved from Research Computing Systems January 2020.

LSTM

Long Short-Term Memory (LSTM) neural networks were chosen for their adept ability of 'remembering' past information. This is done through the cell state of the kernel which is updated as new information is supplied to the model and then passed along to the next time step. This allows LSTM to surpass standard recurrent neural networks where relevant information becomes phased out by new information within a few iterations. The LSTM networks trained utilized 32 hidden units, a batch size of 360, ReLu activation layers, and implemented early stopping to avoid overfitting. The models were trained off of the supplied data discussed in the data section with a cube root normalization, which were supplied in 30 minute segments to predict the next observed geomagnetic field value. Multiple models were made with variations to test the best configuration, these variations include past $d|B_N|/dt$ information in the input parameters to predict absolute value of the geomagnetic field.

Data

To train the model we utilized 15 years of NASA OMNIweb solar wind and SuperMAG data with a 10 minute linear interpolation to fill in small gaps within the solar wind, increasing its volume from roughly 70% coverage to 80% coverage without creating significant periods of interpolated data. From OMNI we focused on IMF magnitude, B_Z , flow speed, flow pressure, ion density, and temperature. SuperMAG provided the ground geomagnetic field for 4 stations across Alaska in a line perpendicular to the auroral oval, which is important for future ionospheric current modeling. To keep MLT dependence within the model, where we see fluctuations in the midnight sector, the MLT of each station was encoded using Sine and Cosine. Lastly, the choice of keeping IMF B_Z as a separate component was to accommodate magnetic reconnection events which are known to be correlated to geomagnetic storms.

Discussion

We found that the best configuration when training LSTM to predict the geomagnetic field was including last known $d|B_N|/dt$ values and training for the absolute value of the field. LSTM is generally trained with the output variable as an input parameter in the dataset, however in testing this results in a function $B(t) = B(t-1)$ as the training converges on the previous geomagnetic field value as the most significant. Further, the original models are trained for $|B_N|$ as this provided the best performance at the cost of sign information, which is a necessary component for ionospheric current modeling. To retain this information, a secondary so-called 'Polarity' model is trained for each station to predict an encoded sign value. The polarity models show promising results with average HSS of 0.92 as seen in Table 1. Further, we can see an increase in HSS within the $d|B_N|/dt$ threshold scores when comparing the original LSTM models predicting $|B_N|$ to the coupled model predicting B_N . The polarity models are adept at persistent positive and negative values, but generally miss a switch in sign by 1 minute. This can be seen within the density plots of Figure 1 where the second and fourth quadrants of the plot show where the coupled model occasionally predicts the wrong sign. In testing this usually correlates to quiet time where the geomagnetic field is fluctuating near 0 nT. As seen in the storm time prediction plots within Figure 1, the polarity model properly calculates the persistent negative enhancement for each station. Within the KAV prediction we can see the model also captures the brief positive fluctuations from the observed dataset around 1500-1800 UTC. While the majority of false predictions occur during quiet time, the storm prediction from CMO shows that in the right conditions the polarity model will provide a false sign swap during a sustained enhancement. There is concern that the coupled model will predict unexpectedly large $d|B_N|/dt$ in this case, however this potential is currently minimized by the base $|B_N|$ model generally underpredicting the magnitude, leading to overall lower values should a false sign switch occur during periods of large $|B_N|$ enhancements.

Results

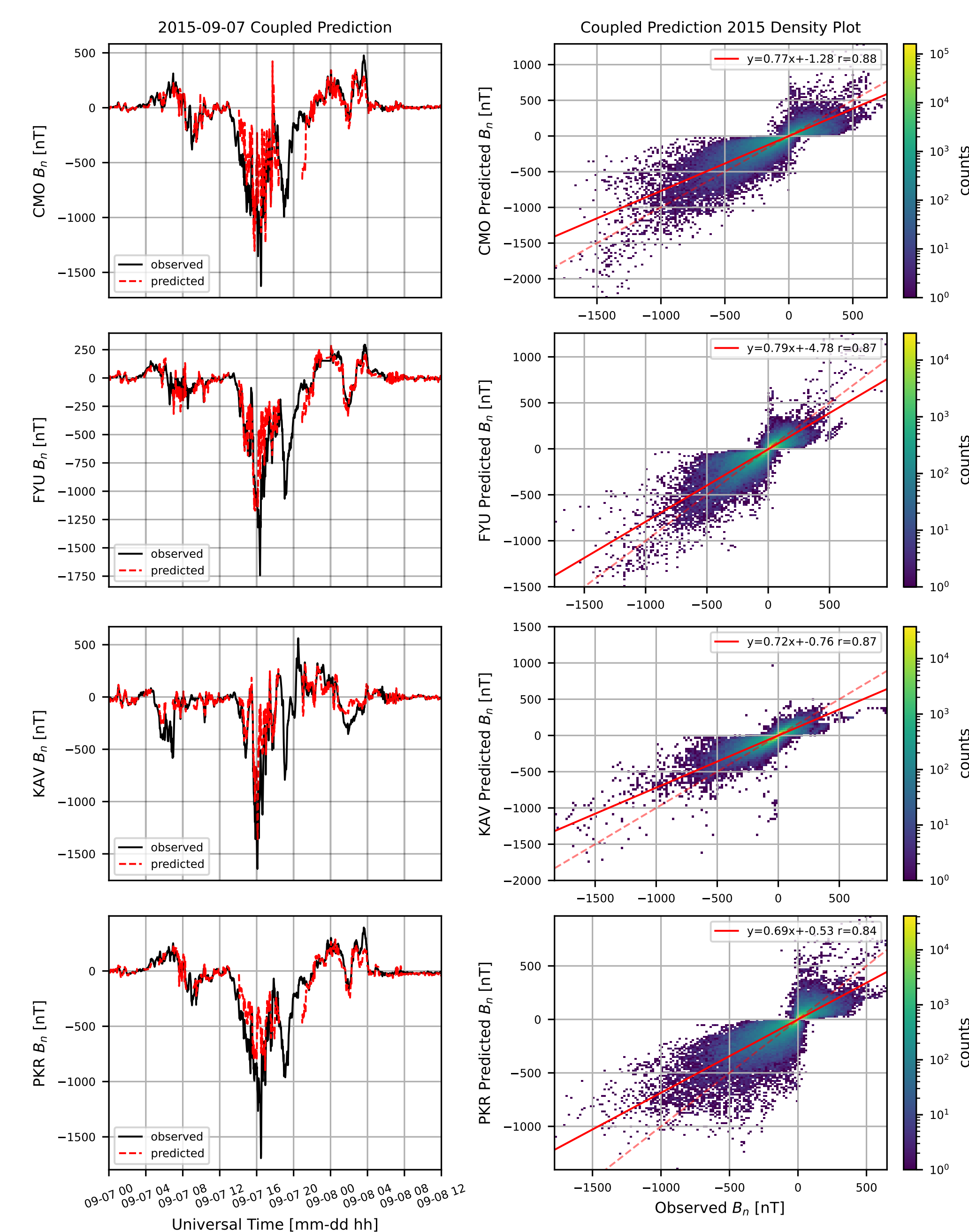


Figure 1: Graphic showing the performance of the coupled model for each station. The left column depicts the Sep-07-2015 storm time prediction of each station while the right columns shows density plots of predicted vs observed values for the year of 2015. The dotted red line corresponds to a perfect prediction while the solid red line is the line of best fit between the predicted and observed values with its Pearson correlation coefficient provided in the legend.

	$d B_N /dt$ [nT/min]				$ B_N $ [nT]			
Threshold	18	42	66	90	14.4	41.6	75.3	427.0
FYU LSTM	0.35	0.28	0.23	0.18	0.48	0.61	0.63	0.58
FYU LSTM (storm)	0.29	0.24	0.26	0.12	0.53	0.70	0.68	0.72
KAV LSTM	0.35	0.29	0.25	0.20	0.58	0.68	0.66	0.50
KAV LSTM (storm)	0.27	0.37	0.23	0.20	0.43	0.54	0.54	0.65
PKR LSTM	0.36	0.26	0.15	0.10	0.39	0.58	0.63	0.47
PKR LSTM (storm)	0.29	0.25	0.27	0.26	0.37	0.76	0.71	0.61
CMO LSTM	0.41	0.31	0.25	0.20	0.68	0.75	0.73	0.60
CMO LSTM (storm)	0.36	0.29	0.28	0.34	0.67	0.74	0.75	0.65
Model	Polarity							
	FYU	KAV	PKR	CMO				
Polarity	0.93	0.90	0.94	0.91				
	$d B_N /dt$ [nT/min]				B_N [nT]			
Threshold	18	42	66	90	14.4	41.6	75.3	427.0
Coupled (FYU)	0.35	0.29	0.23	0.18	0.48	0.61	0.63	0.58
Coupled (FYU) (storm)	0.43	0.35	0.36	0.19	0.61	0.78	0.75	0.72
Coupled (KAV)	0.35	0.29	0.25	0.20	0.58	0.67	0.66	0.50
Coupled (KAV) (storm)	0.37	0.41	0.33	0.28	0.58	0.67	0.61	0.66
Coupled (PKR)	0.32	0.23	0.19	0.15	0.39	0.58	0.63	0.47
Coupled (PKR) (storm)	0.38	0.31	0.36	0.25	0.29	0.81	0.77	0.62
Coupled (CMO)	0.44	0.36	0.30	0.25	0.68	0.75	0.73	0.60
Coupled (CMO) (storm)	0.45	0.46	0.41	0.37	0.77	0.81	0.80	0.67

Table 1: HSS of trained Alaska stations for magnitude $|B_N|$, polarity, and coupled models. Scores are evaluated minute by minute across the year of 2015 and for the 09/07/2015 storm. Polarity has been encoded into a value of 0 (-) or 1 (+) and the HSS corresponds to accurately assessing a 1.

Summary

GICs are a destructive phenomenon that occur during periods of large geomagnetic field fluctuations. In an effort to predict when these extreme fluctuations will happen, an LSTM neural network was trained off of IMF, solar wind, and ground geomagnetic field data. The trained models showed better performance with $d|B_N|/dt$ as in input parameter, bringing a strong significance to global real-time magnetometer data. Further, the models performed best when training with absolute values of the geomagnetic field, leading to a coupled model technique to retrieve the lost sign information. This study aims to find the best performing LSTM and polarity configuration for the values predicted for ionospheric current modeling.